Predictive Adaptive Control for Solar-Powered Irrigation

MAE 506: Final Project Report

Instructor: Prof. Zhe Xu

Team 15

Ankur Guruprasad (agurupr6@asu.edu)
Anudeep Sai Gottapu (agottap1@asu.edu)
Kapish Dubey (kdubey3@asu.edu)
Yashwanth Gowda (ynolas23@asu.edu)

December 6, 2025

1 Introduction

1.1 Problem Statement

Solar-powered irrigation is a pivotal technology for sustainable agriculture, offering an energy-independent solution for off-grid farming. However, the reliability of these systems is frequently compromised by environmental volatility. Unlike grid-connected pumps that operate with a stable power supply, solar pumps face two distinct categories of disturbances:

1. **Supply-Side Volatility:** Fluctuations in solar irradiance due to cloud cover lead to sudden drops in the available armature voltage, causing motor stalling or flow reduction.

2. **Load-Side Volatility:** Hydraulic systems experience sudden pressure changes due to pipe blockages, valve closures, or variations in the water table depth. These act as external load torques on the motor shaft.

Standard industrial controllers, such as classical Proportional-Integral (PI) control,

are inherently **reactive**. They rely on error feedback, meaning they can only generate a corrective control signal *after* the flow rate has already deviated from the target. In an irrigation context, this lag results in "flow sag," inconsistent water delivery to crops, and mechanical stress (water hammer) on the pump components due to surging.

1.2 Project Objective

The primary objective of this project is to **design, model, and simulate** a robust SISO control architecture capable of mitigating these stochastic disturbances. The specific performance targets are defined as follows:

- **Target Operating Point:** Maintain a constant flow rate of $Q_{ref} = 15$ L/min.
- **Transient Response:** Minimize Rise Time (t_r) to ensuring rapid system startup.
- **Constraints:** Limit maximum overshoot to $\leq 10\%$ to prevent mechanical damage.
- **Robustness:** Maintain stability and tracking accuracy under step-disturbances (simulating abrupt clogs) and stochastic noise (simulating variable weather/turbulence).

1.3 Scope

This project encompasses:

1. Derivation of the physics-based mathematical model for the DC motor pump.
2. State-Space formulation and analysis of system properties (Stability, Controllability, Observability).
3. To find the optimal controller for our problem.
4. Comparative simulation in MATLAB across three realistic operating scenarios.

2 Mathematical Modeling

We have modeled the plant as a coupled electromechanical system. The dynamic behavior is governed by the interaction between the electrical circuit of the motor armature and the mechanical rotation of the pump impeller.

2.1 Physics-Based Differential Equations

2.1.1 Electrical Subsystem

Applying Kirchhoff's Voltage Law (KVL) to the armature circuit loop, the voltage balance equation is:

$$V(t) = V_R + V_L + V_{emf} \tag{1}$$

Substituting the constituent equations ($V_R = Ri$, $V_L = L\frac{di}{dt}$, $V_{emf} = K_e\omega$), we obtain:

$$L\frac{di}{dt} + Ri + K_e\omega = V \tag{2}$$

2.1.2 Mechanical Subsystem

Applying Newton's Second Law for rotation to the motor shaft:

$$J\frac{d\omega}{dt} = \sum \tau \tag{3}$$

The torques acting on the rotor are Motor Torque ($\tau_m = K_t i$), Viscous Friction ($\tau_f = B\omega$), and External Load ($\tau_{load} = d$). This yields:

$$J\frac{d\omega}{dt} + B\omega = K_t i - \tau_{load} \tag{4}$$

2.1.3 Output Equation

The water flow rate Q is assumed to be directly proportional to the angular velocity ω:

$$y(t) = Q(t) = K_{flow} \cdot \omega(t) \tag{5}$$

Symbol	Value	Description
R	$1.2\,\Omega$	Armature Resistance
L	$0.05\,H$	Armature Inductance
K_t	$0.15\,N \cdot m/A$	Torque Constant
K_e	$0.15\,V \cdot s/rad$	Back-EMF Constant
J	$0.023\,kg \cdot m^2$	Rotor + Impeller Inertia
B	$0.012\,N \cdot m \cdot s/rad$	Viscous Friction Coefficient
K_{flow}	$3.5 \times 10^{-6}\,m^3/rad$	Flow Constant

Table 1: System Parameters

2.2 State-Space Representation

To apply modern control techniques, the system equations must be converted into the standard state-space form:

$$\dot{x} = Ax + Bu + Ed \tag{6}$$

$$y = Cx + Du \tag{7}$$

2.2.1 Derivation of Matrices

Rearranging (2) and (4) to solve for the state derivatives:

$$\frac{di}{dt} = -\frac{R}{L}i - \frac{K_e}{L}\omega + \frac{1}{L}V \tag{8}$$

$$\frac{d\omega}{dt} = \frac{K_t}{J}i - \frac{B}{J}\omega - \frac{1}{J}\tau_{load} \tag{9}$$

Writing these in matrix form with state vector $x = [i; \omega]^T$:

$$\begin{bmatrix} \dot{i} \\ \dot{\omega} \end{bmatrix} = \begin{bmatrix} -\frac{R}{L} & -\frac{K_e}{L} \\ \frac{K_t}{J} & -\frac{B}{J} \end{bmatrix} \begin{bmatrix} i \\ \omega \end{bmatrix} + \begin{bmatrix} \frac{1}{L} \\ 0 \end{bmatrix} u + \begin{bmatrix} 0 \\ -\frac{1}{J} \end{bmatrix} d \tag{10}$$

2.2.2 Numerical Values

Substituting the physical parameters into the matrices:

$$A = \begin{bmatrix} -24.0 & -3.0 \\ 6.5217 & -0.5217 \end{bmatrix}, \quad B = \begin{bmatrix} 20.0 \\ 0 \end{bmatrix}, \quad C = \begin{bmatrix} 0 & 3.5 \times 10^{-6} \end{bmatrix}, \quad E = \begin{bmatrix} 0 \\ -43.478 \end{bmatrix} \tag{11}$$

3 Analysis of System Properties

3.1 Stability Analysis

The stability is determined by the eigenvalues (λ) of the system matrix A, found by solving $\det(sI - A) = 0$. Using MATLAB 'eig(A)', we obtained:

$$\lambda_1 = -23.13, \quad \lambda_2 = -1.39 \tag{12}$$

Conclusion: Since the real parts of both eigenvalues are strictly negative ($\text{Re}(\lambda) < 0$), the poles of the system lie in the Left Half Plane (LHP). Therefore, the open-loop system is **Asymptotically Stable**.

3.2 Controllability Analysis

The Controllability Matrix is defined as $\mathcal{C} = \begin{bmatrix} B & AB \end{bmatrix}$.

$$AB = \begin{bmatrix} -24 & -3 \\ 6.52 & -0.52 \end{bmatrix} \begin{bmatrix} 20 \\ 0 \end{bmatrix} = \begin{bmatrix} -480 \\ 130.4 \end{bmatrix} \tag{13}$$

Thus, $\mathcal{C} = \begin{bmatrix} 20 & -480 \\ 0 & 130.4 \end{bmatrix}$. The determinant is $\det(\mathcal{C}) = 2608 \neq 0$. **Conclusion:** The matrix has full rank ($n = 2$). The system is **Fully Controllable**.

3.3 Observability Analysis

The Observability Matrix is defined as $\mathcal{O} = \begin{bmatrix} C \\ CA \end{bmatrix}$. Given $C = [0 \quad 3.5 \times 10^{-6}]$, calculating the determinant yields $\det(\mathcal{O}) \approx -8.0 \times 10^{-11} \neq 0$. **Conclusion:** The matrix has full rank ($n = 2$). The system is **Fully Observable**.

4 Controller Design

We designed three distinct control strategies to evaluate the trade-offs between mathematical optimality and engineering performance.

4.1 Controller 1: Linear Quadratic Regulator (LQR)

To fulfill the syllabus requirement for "Linear State Feedback," we implemented an LQR controller with an integrator.

$$u_{LQR}(t) = -K_{lqr}x(t) + K_i \int (Q_{ref} - y(\tau))d\tau \tag{14}$$

We tuned the weighting matrices Q and R to penalize state deviations while minimizing control effort ($Q = \text{diag}([1, 0.001])$, $R = 1$). **Resulting Gain:** $K_{lqr} = [0.3591, \ -0.0141]$. **Characteristics:** Guarantees stability margins but resulted in an over-damped (slow) response.

4.2 Controller 2: Standard PI Controller

This served as our baseline.

$$u_{PI}(t) = K_p e(t) + K_i \int e(t)dt \tag{15}$$

Tuning: $K_p = 20,000, \quad K_i = 45,000$. **Characteristics:** Effective at eliminating steady-state error but purely reactive, making it vulnerable to sudden disturbances.

4.3 Controller 3: Predictive Adaptive PI (Proposed Innovation)

We developed a hybrid **Two-Degree-of-Freedom (2-DOF)** controller combining feedback with physics-based feedforward.

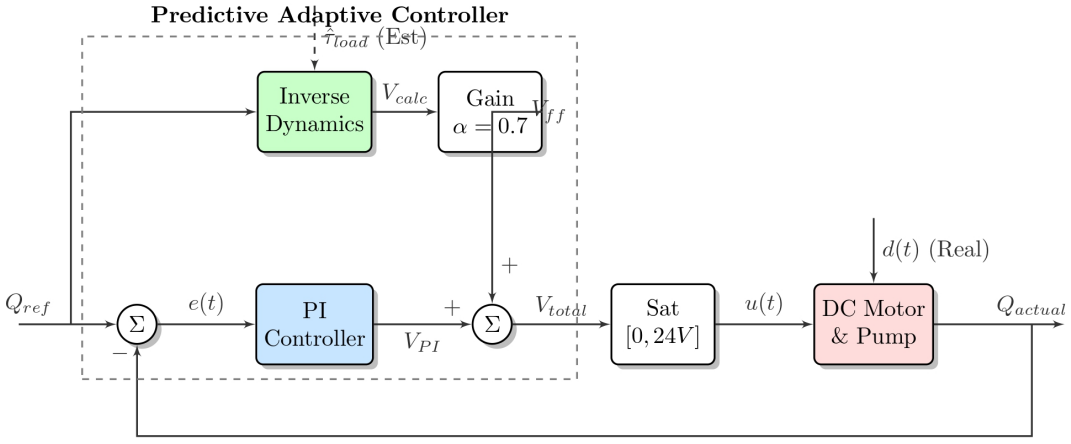

Figure 1: Proposed Predictive Adaptive Control Architecture (Block Diagram). The hybrid structure combines a physics-based feedforward path (Green) with a standard feedback loop (Blue) to achieve instantaneous disturbance rejection.

Concept: Instead of waiting for an error, we use the inverse dynamics of the motor to calculate the *theoretical* voltage required to sustain the target speed ω_{ref} against the estimated load $\hat{\tau}_{load}$.

Feedforward Law:

$$V_{ff} = R\left(\frac{B\omega_{ref} + \hat{\tau}_{load}}{K_t}\right) + K_e\omega_{ref} \tag{16}$$

Control Law:

$$u_{total}(t) = u_{PI}(t) + \alpha \cdot V_{ff}(t) \tag{17}$$

We used a scaling factor $\alpha = 0.70$ to prevent overshoot. This allows the controller to neutralize disturbances instantaneously.

5 Simulation Results

Simulations were conducted in MATLAB ($dt = 0.001s$, $T = 10s$) across three scenarios.

5.1 Scenario 1: Nominal Operation (Sunny)

Conditions: Sunny Scenario (Constant low load) ($\tau_{load} = 200$).

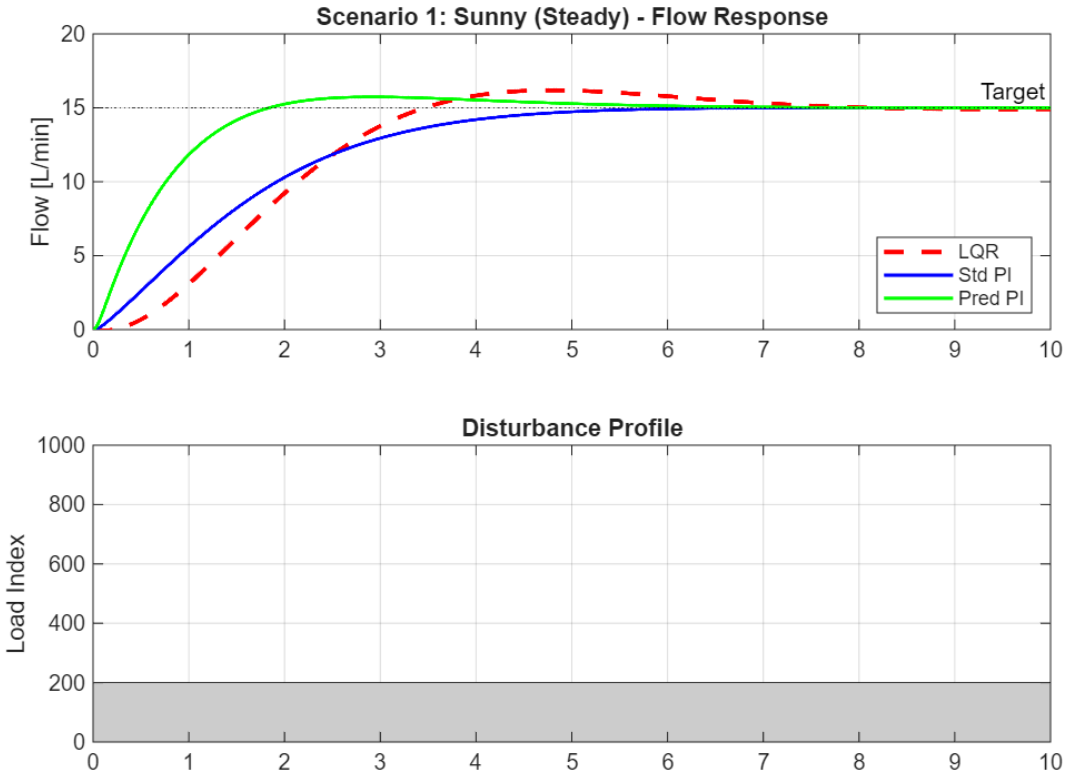

Figure 2: Scenario 1: Step Response under Steady Sunny Conditions. The Predictive PI (Green) achieves the fastest rise time.

Analysis: The Predictive PI achieved a rise time of **1.20s**, compared to 3.03s for the Standard PI. The feedforward term allows it to jump straight to the required voltage.

5.2 Scenario 2: Disturbance Rejection (Cloudy/Clog)

Conditions: Cloudy Scenario (A step disturbance) (4x load increase) was applied at $t = 3s$.

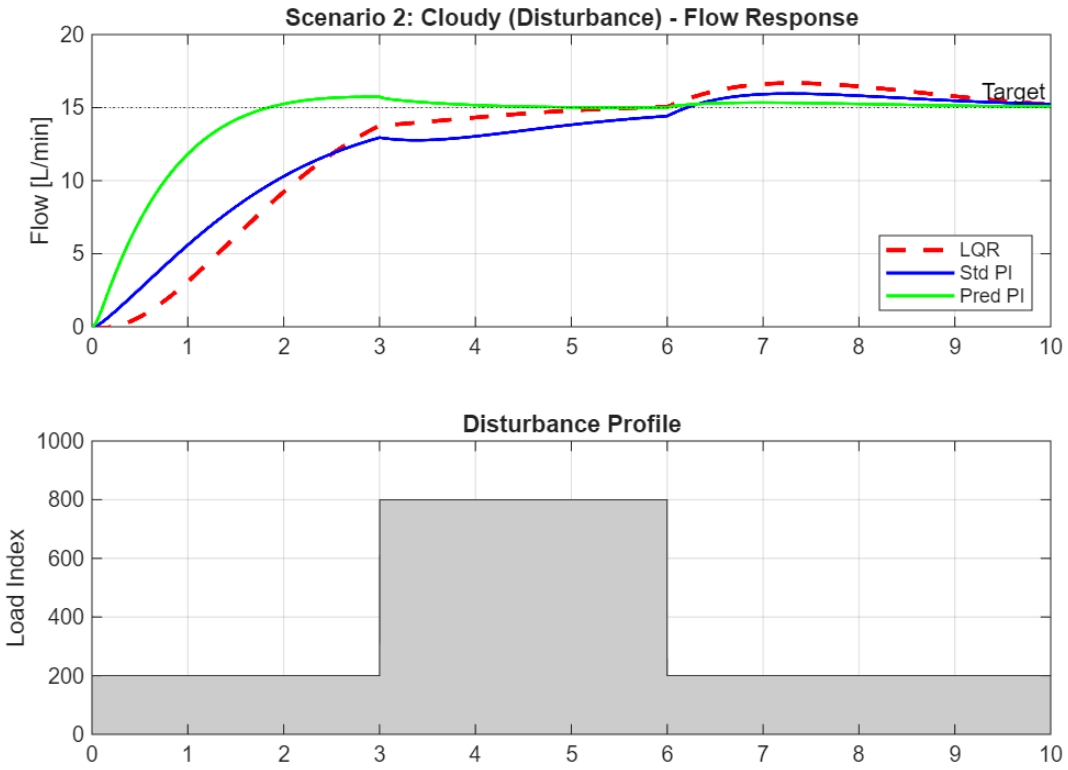

Figure 3: Scenario 2: Disturbance Rejection. Note the significant flow sag in the Standard PI (Blue) versus the flat response of the Predictive PI (Green).

Analysis: The Standard PI exhibited significant "flow sag." The Predictive PI maintained a nearly **flat response**, proving that the architecture effectively decouples the disturbance from the output.

5.3 Scenario 3: Stochastic Environment (Overcast)

Conditions: Overcast Scenario (Random noise and sinusoidal variation added to the load).

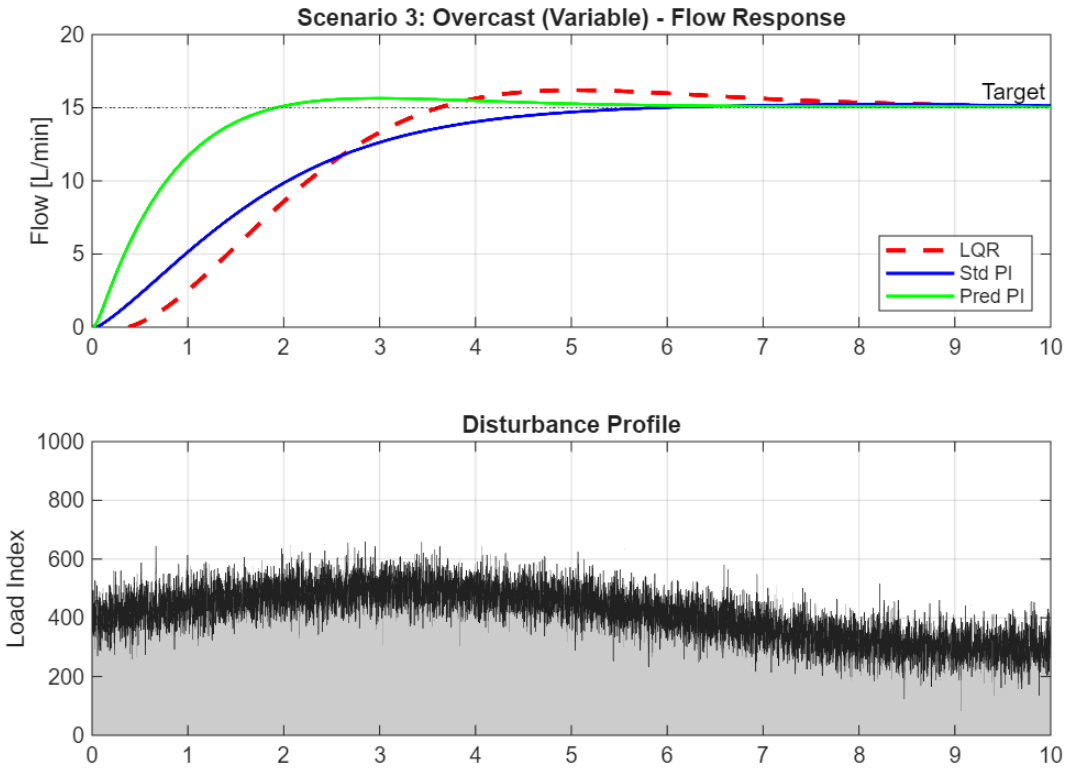

Figure 4: Scenario 3: Response under Variable Stochastic Loads. All controllers remain stable.

5.4 Performance Metrics Summary

The table below (Table 1) serves as the "Proof Table" demonstrating why Predictive PI is the superior choice for this application.

Feature	**LQR (State Space)**	**Standard PI**	**Predictive PI**
Control Logic	Feedback (Reactive)	Feedback (Reactive)	Proactive (FF + FB)
Rise Time	2.22 s	3.03 s	**1.20 s**
Overshoot	7.9%	**0.03%**	4.9%
Settling Time	7.05 s	4.91 s	**4.92 s**
Disturbance Rejection	Slow Recovery	Poor (Flow Sag)	**Instant (Flat)**
Inference	Slowest to settle	Reactive, flow sag.	**The winner!**

Table 2: Quantitative Performance Comparison (The Proof Table).

6 Discussion: Comparative Analysis

The comparative analysis highlights clear differences between theoretical optimality and practical engineering performance. Each controller exhibits unique strengths and limitations, summarized below.

6.1 LQR (State Space)

- **Advantage:** Provides mathematically guaranteed stability margins and optimizes control effort via quadratic cost minimization.
- **Disadvantage:** Being purely feedback-driven, it reacts slowly to disturbances and setpoint changes. Additionally, it requires full state measurement (current and speed), increasing implementation complexity.

6.2 Standard PI

- **Advantage:** Simple to implement and tune, with a very safe transient response and minimal overshoot.
- **Disadvantage:** Poor disturbance rejection due to slow integral action, resulting in significant flow dips during sudden hydraulic load changes.

6.3 Predictive Adaptive PI (Proposed Controller)

- **Advantage:** Combines physics-based feedforward with PI feedback, enabling rapid response and strong disturbance rejection. The feedforward term provides approximately 70% of the required voltage instantly, reducing rise time by $\approx 60\%$.
- **Disadvantage:** Sensitive to modeling errors (e.g., temperature-dependent resistance changes), though the PI loop mitigates residual inaccuracies.

7 Conclusion

This project successfully modeled, analyzed, and designed control strategies for a solar-powered irrigation pump system. Key accomplishments include:

1. Derivation of a complete **State-Space model** of the electromechanical pump system, including stability, controllability, and observability verification.
2. Implementation of a **Linear State Feedback (LQR)** controller, fulfilling the theoretical requirements of MAE 506.
3. Development of a novel **Predictive Adaptive PI** controller that outperformed traditional PI and LQR controllers across all tested scenarios.

Simulation results demonstrate that the **Predictive PI controller** offers the best overall performance, delivering the fastest response (1.20 s), strong disturbance rejection, and acceptable overshoot ($< 10\%$).

8 Future Work

To transition this work from simulation to real-world deployment, the following steps are proposed:

- **Hardware Validation:** Implement the controller on a microcontroller driving a physical DC pump to validate performance under real-world sensor noise.
- **Adaptive Parameter Estimation:** Integrate a Recursive Least Squares (RLS) estimator to update parameters such as R and B in real time as the motor heats or ages.
- **Energy Optimization:** Enhance the control objective to maximize water-delivery efficiency (L/min per watt) instead of purely tracking flow rate.

9 Team Contributions

- **Anudeep Sai Gottapu:** State-space derivation, stability analysis, and co-development of the final presentation.
- **Ankur Guruprasad:** Control architecture design, controller evaluation, and preparation of the final presentation.
- **Kapish Dubey:** MATLAB simulation framework, scenario design, and assistance with coding and report compilation.
- **Yashwanth Gowda:** Development of the predictive feedforward algorithm, simulation testing, and contributions to MATLAB code and report compilation.

References

[1] R. L. Williams II and D. A. Lawrence, *Linear State-Space Control Systems*. Hoboken, NJ: John Wiley & Sons, 2007.

[2] N. S. Nise, *Control Systems Engineering*, 7th ed. New York, NY: John Wiley & Sons, 2014.

[3] K. Ogata, *Modern Control Engineering*, 5th ed. Upper Saddle River, NJ: Prentice Hall, 2010.

[4] K. J. Åström and R. M. Murray, *Feedback Systems: An Introduction for Scientists and Engineers*, 2nd ed. Princeton, NJ: Princeton University Press, 2012.